

Enhancing PySCF-based Quantum Chemistry Simulations with Modern Hardware, Algorithms, and Python Tools

Zhichen Pu^{a)} and Qiming Sun^{b)}

The PySCF package has emerged as a powerful and flexible open-source platform for quantum chemistry simulations. However, the efficiency of electronic structure calculations can vary significantly depending on the choice of computational techniques and hardware utilization. In this paper, we explore strategies to enhance research productivity and computational performance in PySCF-based simulations. First, we discuss GPU acceleration for selected PySCF modules. Second, we demonstrate algorithmic optimizations for particular computational tasks, such as the initial guess manipulation, the second-order self-consistent field (SOSCF) methods, multigrad integration, and density fitting approximation, to improve convergence rates and computational efficiency. Finally, we explore the use of modern Python tools, including just-in-time (JIT) compilation and automatic differentiation to accelerate code development and execution. These approaches present a practical guide for enhancing the use of PySCF’s capabilities in quantum chemistry research.

I. INTRODUCTION

Quantum chemistry simulations play an important role in modern chemistry research. Advancements in software engineering and computing hardware have led to the emergence of a new generation of quantum chemistry computation packages and tools, offering more capabilities in quantum chemistry simulations. Some packages prioritize ease of use by employing user-friendly programming languages like Python, which enhances code readability¹⁻⁸. Some tools leverage advancements in computing models, such as automatic differentiation and tensor contractions, to improve the efficiency of developing new methods⁹⁻¹⁴. Some are optimized for specific hardware, like GPUs, to maximize performance and handle more complex calculations¹⁵⁻²⁰. There are also ongoing efforts to experiment with modern programming languages such as Julia and Rust to incorporate the latest software innovations²¹⁻²⁴.

Balancing performance and simplicity is a challenge in the development of quantum chemistry simulation program. Historically, quantum chemistry packages heavily prioritized performance, often at the expense of code readability and engineering design. Developing such quantum chemistry programs has a high barrier as it requires dedicated efforts and programming skills. For the time being, code readability and program maintainability receive more attention, as the functionalities and methodologies in quantum chemistry become more complicated. With the evolution of programming languages and software engineering concepts, the adoption of object-oriented programming languages like C++ makes programs more modular and manageable. Several quantum chemistry packages, such as ORCA²⁵, MPQC²⁶, Psi4²⁷, Bagel²⁸, and Chronos²⁹, have been written in C++, which has significantly enhanced code readability and maintenance. This shift has made quantum chemistry software more accessible and more suitable for developing complex methods.

Quantum chemistry simulations were used to be treated as black boxes, which is suitable for simple and straightforward

computational tasks. However, as simulation tasks become more complex and demanding, especially when quantum chemistry research integrates with machine learning (ML) techniques³⁰⁻³⁷, tasks such as adjusting programs for hybrid theoretical models, managing computation workflows, and developing effective data processing programs are becoming inevitable. Despite the advancements, the rigidity of C++ quantum chemistry packages often requires users to acquire substantial C++ programming skills, which can pose a significant barrier to entry. In contrast, the Python programming language is renowned for its ease of understanding and learning, making Python programs more straightforward to comprehend and extend. Additionally, due to its popularity in artificial intelligence (AI) development, many attractive tools have been developed by the AI community, granting Python exceptional usability for building scientific computation tools. An increasing number of quantum chemistry tools are adopting Python, and many challenging research projects are being developed and solved using Python code. These trends reflect a shift towards more accessible and flexible programming environments.

PySCF was originally designed to serve this role, offering flexibility for testing new ideas and challenges. To balance simplicity and performance, PySCF was implemented primarily in Python, with performance-critical hotspots optimized in the C language^{1,38}. This is a common design pattern in high-performance Python packages^{1,6,27}. This technology stack enables PySCF to maintain ease of understanding, while still retaining the computational performance for complex quantum chemistry simulations.

When applying PySCF in more chemistry simulation applications, some doubts were raised by users about its computation efficiency and capabilities. Due to the optimization strategies and the API (application program interface) design of the package, the default methods provided by PySCF may not always present the optimal performance. There are various techniques to leverage PySCF’s built-in modules to enhance performance. However, these techniques are not extensively documented in PySCF official documentation, examples, or published papers. Addressing this gap is one of the motivations for writing this paper, which aims to provide a guide for accelerating computations using the functionalities

^{a)}Bytedance Seed

^{b)}Electronic mail: qiming.sun@bytedance.com.; Bytedance Seed

provided by PySCF. This includes the use of GPU acceleration, improved initial guesses, effective self-consistent-field (SCF) convergence strategies, and efficient integral computation routines available in PySCF.

Moreover, PySCF is designed as a Python package rather than standalone software. This design allows PySCF to be seamlessly integrated into any existing Python infrastructure. PySCF can be used with various Python tools to enhance its capabilities. The functionalities provided by the Python community offer broader ways to improve the productivity of quantum chemistry simulations. This is another point we aim to illustrate in this work.

In this paper, we will discuss several techniques to enhance the productivity of the PySCF package. Section II briefly reviews the functionalities of PySCF package and its ecosystem. Section III demonstrates how to accelerate computations using the PySCF GPU extension. Section IV discusses how to improve computation efficiency using functionalities provided by the PySCF package. Section V explores how PySCF can be combined with just-in-time compilation and automatic differentiation techniques.

II. OVERVIEW OF PYSCF

A. Features provided by PySCF

PySCF is an open-source Python package for solving electronic structure problems using Gaussian-type basis sets. It supports both molecular systems and extended systems with periodic boundary conditions. Key features and functionalities of PySCF include:

- Mean-field energy, gradients, and Hessian.
- Single-reference post-Hartree-Fock methods such as Møller-Plesset perturbation, coupled cluster, and Random phase approximation (RPA) methods.
- Multi-configurational and multi-reference methods for electron correlation.
- Excited states modelled by density functional theory, equation-of-motion coupled cluster, and ADC (Algebraic Diagrammatic Construction) methods.
- Various molecular properties calculations.
- Scalar relativistic, two-component and four-component relativistic effects.
- Solvent effects through implicit solvent models.
- DFT and post-HF methods for extended systems with periodic boundary condition.

B. PySCF Eco-system

The PySCF package is organized into core modules, PySCF-Forge, and various extensions. The core module

provides the fundamental functionalities required for quantum chemistry simulations. Within this module, settings and strategies are implemented conservatively, with tight thresholds to ensure accurate and reliable results. The implementation of the PySCF core module focuses on functional programming, lightweight design yet efficient performance.

Newly developed methods are available in PySCF-Forge, which serves as a staging area for future features in PySCF. GPU acceleration is implemented in the GPU4PySCF package^{15,18}, which is specifically designed to enhance performance. The use of GPU4PySCF with PySCF will be discussed in Section III. Another significant extension is PySCFAD⁹, which extends PySCF by providing automatic differentiation capabilities for all methods in PySCF. These are the primary extensions of PySCF. Additional extensions, which may be written in different languages or managed at different levels of maintenance, are available on the PySCF organization page on GitHub. We will not list all of them in this paper. The core module, PySCF-forge and these extensions constitute the PySCF ecosystem.

C. PySCF APIs

PySCF is designed as a Python package. Unlike traditional quantum chemistry packages, which typically use a DSL (domain specific language) configuration file through a driver, PySCF provides APIs to execute its functionalities directly in Python.

Quantum chemistry methods are implemented as classes, organized in the object-oriented programming (OOP) structure. To perform a quantum chemistry task, one can instantiate a `Mol` object, apply the classes corresponding to the desired methods, and then call the `.run()` method to execute the computation. For example

```
mol = pyscf.M(atom='''
O  0.  0.000  0.118
H  0.  0.755 -0.471
H  0. -0.755 -0.471''',
basis='cc-pvdz')
mol.RKS(xc='pbe0').run()
```

Subsequent methods can be chained together to streamline computations. For instance, the time-dependent density functional theory (TDDFT) methods and their gradients can be executed sequentially:

```
mf = mol.RKS(xc='pbe0').run()
mf.TDDFT().run().Gradients().run()
```

Parameters for each method can be specified as keyword arguments when calling the `.run()` method, or be assigned directly to each instance, just like manipulating the attributes of a class in OOP programming. For example, the following two setups are equivalent:

```

# Supply parameters as keyword arguments
mol.RKS(xc='pbe0').run().TDDFT().run(nstates=6, triplet=False).Gradients().run()
# Assign parameters to attributes
mf = mol.RKS()
mf.xc = 'pbe0'
mf.run()
td = mf.TDDFT()
td.nstates = 6
td.triplet = False
td.run()
td_grad = td.Gradients()
td_grad.run()

```

Additional features, such as solvent model, relativistic corrections, can be applied within the chain call as well. For example, the PCM solvent model are attached to the DFT calculation and subsequently applied to the TDDFT excited state computation:

```
mol.RKS(xc='pbe0').PCM().run().TDDFT().run()
```

The solvent model is applied to the RKS method. Its effects influence the ground state wavefunction (the DFT orbitals), as well as the subsequent TDDFT response calculation. If the application order is altered,

```
mol.RKS(xc='pbe0').run().TDDFT().PCM().run()
```

the orbitals from gas phase will be used in the linear response computation. Although the solvent model will still contribute to the linear response matrix, the results will be different from those obtained using the RKS-PCM-TDDFT combination. Unlike writing configuration in the input file where feature keywords are simply listed, the order in which methods are applied matters using the chain execution APIs.

The second type of APIs in PySCF are individual functions. They provide independent features that do not belong to a specific simulation method. A typical example of this category is the integral evaluator function. The common API `mol.intor()` method supports the evaluation of various types of integrals. The `pyscf.scf.jk.get_jk()` function is another example, which provides the general function to compute Coulomb and exchange matrices. It supports an arbitrary number of density matrices and any two-electron integrals implemented by the Libcint library³⁹, including zeroth-order, high-order derivatives, or Gauge-included two-electron integrals, across multiple molecules. For more details on these functions, please refer to the PySCF online documentation at www.pyscf.org.

III. GPU ACCELERATION

To maintain functional generality and ease of modification, the default algorithms and engineering practices in PySCF may not be optimized for peak performance. Additionally, to decrease numerical uncertainty, various thresholds in PySCF are set very tight. These choices lead to slower execution for certain functionalities when using the default code in PySCF,

compared to other packages. To address this problem, one method is to select different algorithms than the default one, which will be discussed in Section IV. Another option is to switch to the more efficient package, GPU4PySCF, to achieve faster execution.

The GPU4PySCF extension is developed with a priority on performance optimization. As the name indicates, the package leverages GPU hardware to improve the processing of computationally expensive workloads. This includes the implementation of various integral computation algorithms on GPU and the use of GPU tensor libraries for linear algebra operations. When designing algorithms and their implementations, this extension prioritizes performance-oriented variants. The code readability and the generality of features may not be as emphasized as they are in PySCF core modules.

At the current stage, the GPU4PySCF package primarily focuses on accelerating DFT computations. The most significant performance improvements are observed in two areas. The first is DFT calculations for medium-sized molecules (50 - 100 atoms). The second area is in handling large molecules that involve over 10,000 basis functions. For medium-sized molecules, the density fitting approximation is employed. Thanks to the substantial advantages of tensor contraction operations on GPUs, GPU4PySCF can achieve speedups of 2 - 3 orders of magnitude over traditional CPU-based code¹⁵.

When it comes to molecules that contain over 1,000 atoms, or more than 10,000 basis functions, performing standard DFT calculations becomes a significant challenge for many CPU-based programs. Even if computationally feasible, the time required to complete these calculations is impractical for routine tasks. In the case of GPU programs, although GPUs offer substantial computational capabilities, there are technical challenges in performing these large-scale calculations on GPUs. The density fitting approximation is not feasible due to its high scaling when evaluating the HF exchange matrix. Integrals must be evaluated on the fly during the SCF iteration. In this context, various analytical integral algorithms have been intensively optimized within the GPU4PySCF package for the calculation of Coulomb and exchange matrices¹⁸. The technical details of the program implementation are beyond the scope of this paper. More details will be presented in our upcoming works.

The GPU4PySCF APIs generally follows the APIs provided by the PySCF package, including the naming conventions, the order of parameters, the keyword arguments in

function signatures. GPU4PySCF also implements Python classes to represent the individual quantum chemistry methods using the same name as those in PySCF core, as well as the parameters and attributes within each method class. This design allows users to seamlessly replace the PySCF core implementations with those of GPU4PySCF in a straightforward manner. For instance, the restricted Kohn-Sham DFT method in the PySCF core module is available at `pyscf.dft.RKS()`. In GPU4PySCF, this method is accessible as `gpu4pyscf.dft.RKS()`. To perform a RKS calculation using GPU4PySCF, the script can be written following the PySCF APIs:

```
from gpu4pyscf.dft import RKS
RKS(mol, xc='pbe0').run()
```

To simplify the conversion between GPU4PySCF and PySCF objects, two methods, `.to_gpu()` and `.to_cpu()`, have been introduced in PySCF and GPU4PySCF classes respectively. For an instance created by PySCF code, the `.to_gpu()` method recursively transforms the PySCF instance and its attributes to objects suitable for GPU acceleration. After executing the computation on GPU, the object can be transformed back to the instance of the PySCF core modules, simplifying the subsequent CPU operations. For example, we can execute the computationally intensive TDDFT diagonalization on GPU and then analyze the TDDFT response coefficients using the functionalities provided by the PySCF core on CPU.

```
tddft_on_gpu = mol.RKS().to_gpu().run().TDA()
tddft_on_gpu.to_cpu().analyze()
```

In addition to the classes for individual simulation models, GPU4PySCF also offers several functions to accelerate the demanding functions implemented in PySCF, particularly those for integral computation. For example, the `get_jk` function in the `gpu4pyscf.scf.hf` module can efficiently evaluate the Coulomb matrix and exchange matrices for any given density matrices.

```
from gpu4pyscf.scf.hf import get_jk
jmat, kmat = get_jk(mol, dm)
```

This function can work as a drop-in replacement to the `get_jk` function of the `pyscf.scf.hf` module. Another example is the numerical integration functions provided by the `gpu4pyscf.dft.numint` module. In this module, density evaluation and integral computations functions for various types of exchange-correlation (XC) functionals have been implemented using custom GPU kernels and tensor contraction code on GPU. The numerical integration features in PySCF can also be enhanced using these accelerated functions.

```
from gpu4pyscf.dft.numint import NumInt
rho = NumInt().get_rho(mol, dm, grids)
```

Other function-level acceleration features include the evaluation of three-center integrals and their derivatives, grid-based Coulomb integral evaluation in the implicit solvent model, the calculation of the Coulomb interaction matrix between the

quantum mechanical (QM) region and molecular mechanics (MM) particles in the QM/MM model⁴⁰, and the multigrid algorithm for DFT XC integrals. These functions can also be utilized to accelerate specific functions within the corresponding core modules of PySCF.

To minimize the overhead associated with data transfer between CPU and GPU architectures, GPU4PySCF functions tend to store large-sized arrays, such as wave-function coefficients, density matrices, and integrals, in CuPy arrays. Using NumPy code to manipulate these CuPy arrays can lead to compatibility issues. Therefore, when PySCF core functions are used to handle data generated by GPU4PySCF, it is important to explicitly convert the data types of GPU4PySCF outputs using the CuPy function `cupy.asnumpy()`.

IV. METHODS AND ALGORITHMS TO IMPROVE PYSCF PERFORMANCE

A. Manipulating Initial Guess

The initial guess is crucial in electronic structure simulations. The quality of the initial guess can significantly impact the computational performance and the correctness of the results.

The method classes in the PySCF package generate the default initial guess based on established experience. It also allows users to construct their own initial guesses and pass them to each computational method. In PySCF, custom initial guesses for mean-field methods, post-Hartree-Fock methods, and excited state methods are handled in three separate approaches.

1. Initial Guess for Mean-field Methods

For mean-field methods, the initial guess can be provided as a density matrix through the `.kernel()` method:

```
mf = mol.RKS(xc='pbe0')
mf.kernel(dm0=initial_guess_density_matrix)
```

The density matrix for an initial guess does not necessarily originate from a single determinant. There is no need to consider whether the density matrix obey the idempotent property or yield the correct number of integer electrons. It can be constructed simply to reflect specific chemical intuition or the locality of the chemical system.

To customize the initial guess density matrix, it is necessary to know how the basis functions are ordered, as different software packages adopt different conventions. To eliminate any ambiguity in the order of basis functions, the PySCF package offers several APIs to help users identify the atomic character of the basis functions. The `.ao_labels()` method of the `Mole` class provides the labels of each basis function, such as `'1 C 4py'`. The three components in the output represent the atom ID, the symbol of the element, and the basis notation, respectively. The `.search_ao_label()` method of the `Mole` class returns the indices of the basis functions

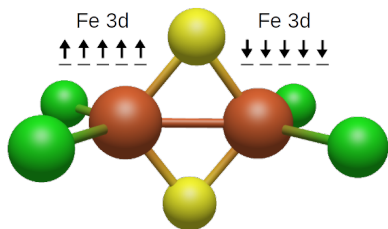


FIG. 1: The electron spin are customized in the initial guess for the Fe atoms in the $\text{Fe}_2\text{S}_2\text{Cl}_4$ molecule.

that match the specified regular-expression pattern. For example, `mol.search_ao_label('C.*pz')` would search for all p_z type atomic orbitals (AO) associated with Carbon atoms within the molecule. The following example demonstrates how to use these functions to construct a spin-symmetry broken initial guess for the two Fe atoms in an iron-sulfur molecule, as shown in Figure 1.

```
mf = mol.UKS(xc='pbe')
dma, dmb = mf.get_init_guess()
fe0_3d = mol.search_ao_label('0 Fe 3d')
fe1_3d = mol.search_ao_label('1 Fe 3d')
dma[fe0_3d[:,None], fe0_3d] = np.eye(5)
dmb[fe1_3d[:,None], fe1_3d] = np.eye(5)
dma[fe1_3d[:,None], fe0_3d] = 0
dmb[fe0_3d[:,None], fe1_3d] = 0
mf.kernel(dm0=np.array((dma, dmb)))
```

Another effective practice for setting up the initial guess in mean-field calculations is to project the initial guess from the results of a smaller-scale, preliminary calculation. This approach is particularly useful in potential energy surface scans and geometry optimization. In these scenarios, one simply constructs the density matrix from a previous calculation using the `.make_rdm1()` method, and then passes it to the next calculation.

When handling challenging systems such as gapless systems, ions with diffused basis functions, or transition metal complexes with various spin-polarized local minima, convergence issues may arise in regular SCF iterations. In these scenarios, we can first converge the calculation using a small basis set (such as the DZ basis set without diffused functions) and a different functional (such as UHF). The results can then be projected to larger basis sets using the `project_dm_nr2nr()` function from the `pyscf.scf.addons` module. For example,

```
from pyscf.scf.addons import project_dm_nr2nr
dma_dz, dmb_dz = mol_dz.UHF().run().make_rdm1()
dma_tz = project_dm_nr2nr(mol_dz, dma_dz, mol_tz)
dmb_tz = project_dm_nr2nr(mol_dz, dmb_dz, mol_tz)
mf = mol_tz.UKS(xc='pbe')
mf.kernel(dm0=(dma, dmb))
```

If both the basis set and the geometry of the target system differ from those used in the preliminary calculation, the projection should be performed between the different basis sets

while keeping the geometry unchanged. The resulting density matrix can then be directly utilized in the full-sized problem. Projecting the density matrix between molecules with different geometries should be avoided. Doing so would result in the density matrix on the new geometry representing the electron density of the old geometry, which would be an inappropriate initial guess. This should be avoided.

2. Initial Guess for Post-Hartree-Fock Methods

The initial guess for post-Hartree-Fock methods, particularly the configuration interaction (CI) family, requires a different format of initial guess. Typically, the CI coefficients are derived from the MP2 amplitudes, which are generally sufficient for initializing both CI and coupled cluster (CC) methods.

Preparing the initial guess for multi-configurational self-consistent field (MCSCF) calculations is a special case. It requires to supply both the orbitals and the wavefunctions of the active space solver (by default, the FCI solver). In most scenarios, supplying an initial guess for the active space solver is not necessary, as it has relatively little impact on the results of the MCSCF problem. In contrast, the initial orbitals play a crucial role in MCSCF calculations. A proper set of initial orbitals not only accelerates convergence but also influences the correctness of the results. Various methods have been explored for constructing MCSCF initial orbitals^{41–47}.

The most straightforward approach is to select specific orbitals from the preceding Hartree-Fock calculations. The `.sort_mo()` method of the MCSCF classes in PySCF (including CASCI and CASSCF and the derived state-average MCSCF classes) provides the basic functionalities for this task. Another common strategy for the MCSCF initial guess is the use of natural orbitals from UKS or MP2 calculations. For unrestricted Kohn-Sham (UKS) calculations, the spin-traced density matrix can be computed. The SciPy diagonalization routine can then be used to obtain the natural orbitals:

```
mf = mol.UKS().run()
dma, dmb = mf.make_rdm1()
dm_sf = dma + dmb
nat_occ, nat_orb = scipy.linalg.eigh(
    dm_sf, mf.get_ovlp(), type=2)
nat_occ = nat_occ[:, :-1]
nat_orb = nat_orb[:, :-1]
```

For MP2 calculations, it should be noted that the MP2 density matrix is computed by default in the molecular orbitals (MO) representation. When calling the `make_rdm1()` method of the MP2 classes, the option `ao_repr=True` should be specified to ensure that the density matrix is output in the AO representation. The subsequent steps for obtaining the natural orbitals are the same as the UKS case.

More sophisticated orbital initial guess can be constructed using the PySCF built-in modules APC, AVAS, and `dmet_cas`. The APC (approximate pair coefficient) method⁴¹ selects active space based on the order of APC entropy, which is a measure of the interaction between the virtual orbitals and the oc-

cupied orbitals based on the exchange matrix. The following code example can be utilized to generate active space as well as the initial orbitals:

```
myapc = apc.APC(mf, max_size=12)
ncas, nelecas, mo_init_guess = myapc.kernel()
mc = mf.CASSCF(ncas, nelecas)
mc.run(mo_coeff=mo_init_guess)
```

This APC initial guess remains the use of canonical mean-field orbitals. When handling transition metal complexes, the active center are typically chosen to the *d*-shell of the transition metal. One would like to construct the active space to in-

```
ncas, nelecas, mo_init_guess = dmet_cas.guess_cas(mf, mf.make_rdm1(), 'Fe 3d')
mc = mf.CASSCF(ncas, nelecas)
mc.run(mo_coeff=mo_init_guess)
```

The `dmet_cas` function requires to specify the orbitals of interest using their atomic labels, such as "Fe 3d", as the primary components of the active space. This function uses these labels to identify atomic orbitals (using the `mol.search_ao_label()` method). It then decomposes the density matrix with respect to these atomic orbitals to extract their entangled bath orbitals. The specified atomic orbitals along with the entangled bath form the active space.

3. Initial Guess for Excited States

By default, the initial guess for excited states is constructed based on the energy gap between occupied and virtual orbitals. To solve N excited states, the N single orbital-pair excitations with the smallest occupied-virtual energy differences are selected as the initial guess.

A common issue with this initial guess construction is that it may overlook certain low-lying excited states. The initial N states might not include the symmetry sectors of these low-lying excited states. Consequently, these states are completely

```
td = mf.TDA().run(nstates=10)
cc = mf.CCSD().run()
eom = cc.EOMEESinglet()
n = eom.vector_size()
nocc, nmo = cc.nocc, cc.nmo
nvir = nmo - nocc
r2 = np.zeros((nocc, nocc, nvir, nvir))
nstates = 3
guess = [eom.amplitudes_to_vector(x, r2) for x, y in td.xy[:nstates]]
eom.kernel(nstates, guess=guess)
```

Both TDDFT and EOM-CC-CCSD in PySCF support singlet, triplet, and spin-flip computations. Similar transforma-

clude the atomic characteristic orbitals of the active transition metal. In such cases, the active space could be constructed using the orbitals from the transition metal, supplemented by ligand orbitals based on their entanglement with the orbitals of the transition metal. The density-matrix embedding theory (DMET) based scheme, including the AVAS (atomic valence active space)⁴⁵ and `dmet_cas` were developed to address this need. The AVAS and `dmet_cas` selection schemes are largely interchangeable, with minor difference in the treatment of open-shell electrons. Here, we demonstrate the use of `dmet_cas` for this category:

excluded from the subspace spanned by the Davidson diagonalization iterations, and thus, they are not represented in the results.

One effective approach to address this problem is to compute more states than the required number, hoping that the enlarged initial space could potentially include more symmetry sectors. However, this approach increases the computational costs, particularly for the CI and equation-of-motion CC (EOM-CC) computations. These methods demand substantial CPU resources, memory usage, and I/O storage, all of which scale proportionally with the number of states being computed.

To reduce the computation costs, we can convert the TDDFT results to the initial guess for these methods, assuming the TDDFT is more cost effective. The example below demonstrates how to first perform a singlet TDDFT computation and then use the TDDFT results as the initial guess for a singlet type of EOM-CC-CCSD. The initial guess for EOM-CC consists of a flattened vector containing single and double excitation coefficients. Only the X amplitudes from the TDDFT results are used to replace the single excitation coefficients.

tions can be applied to triplet and spin-flip computations as well. Details for these conversions are not demonstrated here.

B. Second-Order Self-Consistent Field (SOSCF) Convergence

The second order SCF (SOSCF) algorithm in PySCF⁴⁸ is an exact second-order solver that computes the orbital Hessian precisely. Originally, it was not designed to reduce the computation timing for arbitrary inputs. Instead, it focuses on ensuring convergence to a local minimum solution that is close to the provided initial guess. Unlike the quasi-newton implementations in other packages^{49–52}, it does not employ aggressive optimization techniques, such as line search or extensive trust region strategies, to reduce the number of iterations.

For simple systems with large orbital energy gaps, SOSCF may not necessarily outperform the default DIIS (direct inversion in the iterative subspace) scheme. However, as an exact second-order solver, it exhibits advantages by achieving quadratic convergence when the initial guesses that are close to a local minimum. For challenging systems, such as transition metal complexes, open-shell systems, dissociated molecules, or systems with small HOMO-LUMO gaps, switching to the SOSCF solver after several DIIS iterations often yields better performance than using the DIIS algorithm throughout the entire convergence process.

To enable an SOSCF calculation, we can invoke the `newton` method to create an SOSCF instance. Please note that the SOSCF instance is independent from the original mean-field instance. Solving the mean-field wavefunction using the SOSCF instance does not alter the original mean-field object (due to the side-effect free design of PySCF).

```
# This mf object utilizes DIIS algorithm
mf = mol.UKS(xc='pbe')
# Create an independent SOSCF object
soscf_mf = mf.newton()
soscf_mf = soscf_mf.run()
mf = soscf_mf.undo_newton()
```

The `undo_newton()` method, called at the end, reverts the SOSCF instance back to the regular mean-field instance. This conversion can be omitted if the mean-field instance is subsequently used for post-HF calculations. This conversion is automatically applied within the post-HF methods in PySCF.

Given that the SOSCF method in PySCF is not optimized for calculations starting from poor initial orbitals, it is advisable to perform a fast preliminary computation first. This preliminary step could be performed with approximate integrals (Section IV C), different functionals, or even a different basis set. When a different basis set is used, the density matrix from the preliminary computation should be projected, as discussed in Section IV A 1, and then supplied to the SOSCF kernel function.

The SOSCF method depends on the orbital Hessian, which is the most computationally demanding operation in the SOSCF process. PySCF allows the use of approximate integrals for the orbital Hessian, while the total energy and orbital gradients are evaluated using exact integrals. Although the approximate orbital Hessian may slightly affect the convergence performance, the final converged results remain unchanged, as

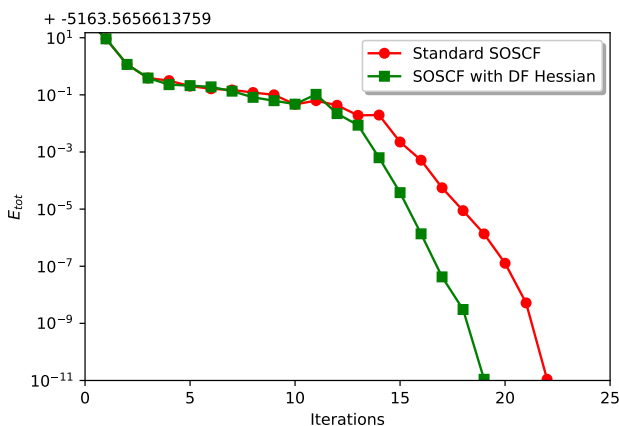


FIG. 2: Convergence rate comparison between standard SOSCF and SOSCF with approximate DF orbital Hessian.

the total energy and orbital gradients are computed accurately. The following example demonstrates the use of density fitting integrals to approximate the orbital Hessian in SOSCF.

```
mf = mol.UKS(xc='pbe0')
mf = mf.newton()
# DF approximate integrals for orbital Hessian
mf = mf.density_fit()
mf = mf.run()
```

Figure 2 illustrates the convergence rate of the SOSCF for a challenging system (the iron-sulfur molecule in Figure 1). The calculations were performed using the PBE0 functional with the def2-TZVP basis set. The initial guess for this test was constructed from the spin-polarized density matrix, as shown in Figure 1. This was not an optimal initial guess for this particular case. Initially, the decrease in energy is slow. As the solver approaches the local minimum, it exhibits rapid convergence. The auxiliary basis set (ABS) def2-universal-jfit⁵³ is used in the DF approximate orbital Hessian. This ABS is not considered suitable for standard DFT calculations when using hybrid functionals. Despite this, the DF approximate orbital Hessians performs exceptionally well. The convergence speed of SOSCF using the approximate orbital Hessian and the exact Hessians is essentially identical.⁴⁸

C. Approximate Integral Computation

In many quantum chemistry calculations, particularly the mean-field level theory, integral computation dominates the computation works. Altering the integral computation algorithm could improve computation efficiency. PySCF offers several integral algorithms to accelerate the evaluation of exchange-correlation (XC) functional numerical integration, the Coulomb matrix, and the HF exchange matrix.

1. Multigrid Integration

The numerical integration of XC functionals can be significantly accelerated using the multigrid integration algorithm. The multigrid algorithm for XC functional integration was originally developed by the CP2K program package⁵⁴. This algorithm was introduced into PySCF 1.6 with adaptations to the PySCF code structure and enhanced control of numerical precision. Recently, the algorithm has been carefully optimized and migrated to the GPU architecture, and is currently under development in the GPU4PySCF package⁵⁵. The advantages of the multigrid algorithm, including its recent developments, will be further detailed in upcoming publications⁵⁶.

The multigrid algorithm leverages the locality of Gaussian basis functions to reduce computational efforts in numerical integration. It is specifically tailored for uniform integration grids. Uniform grids are not as effective as Becke atomic

grids in handling core electrons near the nuclei. Very dense grids are required to accurately describe the electron density of core electrons. However, these dense grids can lead to exceptionally large memory usage, and a very high cost for the discrete Fourier transforms that the multigrid algorithm relies on. Except for light elements, the multigrid algorithm is generally not used directly for all-electron calculations. Rather, it is typically combined with pseudo-potentials to screen the core electrons.

The PySCF periodic boundary condition (PBC) DFT program employs uniform grids for integration evaluations. The multigrid can be naturally applied to PBC computations. However, the multigrid program is not compatible with the default Becke grids scheme used by the PySCF molecular DFT code. Additional setup steps are necessary for molecular systems. The example below illustrates how to configure the multigrid algorithm for a molecule cluster:

```
# 1. Mole object for the water cluster. Pseudo potentials are applied to screen core
  electrons.
mol = pyscf.M(atom='xyz-of-cluster', basis='gth-tzvp', pseudo='gth-pbe')
# 2. Define a box large enough to include all electron density of the molecule
box = np.eye(3) * 30
# 3. Convert the Mole object to a Cell object. Setting dimension=0 to screen
# Coulomb interactions between periodic images
cell = mol.to_cell(box=box, dimension=0)
# 4. Replace the default numerical integrator with the MultiGridNumInt class for DFT
  instance
mf = cell.RKS(xc='pbe')
mf._numint = multigrid.MultiGridNumInt(cell)
# 5. Adjust mesh to refine the size of uniform grids.
mf._numint.mesh = [105, 105, 105]
mf.run()
```

In this code snippet, we intentionally demonstrates how to convert between a Mole instance and a Cell instance using the `.to_cell()` method. However, the first three steps can be combined by directly instantiating a Cell class with the box and the `dimension=0` setting. To ensure that the PBC-based DFT computation numerically matches the molecular DFT results, the `dimension=0` setting is necessary.

Adjusting the multigrid mesh can reduce computation costs, though it results in a trade-off in integration accuracy. During each step of the SCF iterations, the package can display the number of electrons calculated from the multigrid integration. This output can be used as an indicator of the error introduced by the truncated mesh.

Although the multigrid may introduce certain errors in the description of core electrons, it remains a valuable tool for accelerating all-electron DFT simulations in various ways. The multigrid can be used for preliminary computations to gener-

ate an initial guess. When combined with the Second-Order Self-Consistent Field (SOSCF) method, it can be used to approximate the orbital Hessian. The code snippet below shows the use of the multigrid algorithm with the SOSCF method.

```
mf = mol.RKS(xc='pbe')
cell = mf.to_cell(box, dimension=0)
mf = mf.newton()
mf._numint = multigrid.MultiGridNumInt(cell)
mf._numint.mesh = [105, 105, 105]
mf.run()
```

2. Density fitting

The density fitting (DF) method, also known as the resolution-of-identity (RI) method, employs a three-index tensor to approximate four-center two-electron integrals⁵⁷

$$(\mu\nu|\kappa\lambda) = \int \chi_\mu(\mathbf{r}_1)\chi_\nu(\mathbf{r}_1)\frac{1}{r_{12}}\chi_\kappa(\mathbf{r}_2)\chi_\lambda(\mathbf{r}_2)d\mathbf{r}_1d\mathbf{r}_2 \approx \sum_P T_{P,\mu\nu}T_{P,\kappa\lambda} \quad (1)$$

Here, $\chi(\mathbf{r})$ denotes the orbital basis functions. The index P corresponds to the auxiliary basis functions $\chi_P(\mathbf{r})$ which are utilized to construct the T tensor,

$$M_{PQ} = (\chi_P|\chi_Q) = LL^T, \quad (2)$$

$$T_{P,\mu\nu} = \sum_Q (L^{-1})_{PQ} (\chi_Q|\mu\nu). \quad (3)$$

For small or medium-sized molecules, using this integral approximation has several advantages:

- It is more efficient than the traditional analytical method of computing four-index integrals.
- It requires less memory storage and it reduces I/O pressure.
- It offers reduced scaling in the AO to MO integral transformation.

As a result, the DF approximation significantly enhances the performance in the computation of Hartree-Fock exchange and various electron-correlation methods. It has been adopted as the default in many software packages (such as Psi4, ORCA, Bagel). However, PySCF does not set it as the default computation scheme.

In PySCF, the DF approximation can be manually enabled for various methods, including Hartree-Fock, DFT, MCSCF, MP2, and CCSD. For mean-field methods, the `.density_fit()` method can be used to create DF mean-field instances. Based on a DF mean-field instance, calling its shortcut methods such as `.CASCI()` and `.CASSCF()` will inherit the DF approximation in these subsequent post-HF calculations. However, as of PySCF 2.9, the package does not provide similar shortcuts for other post-HF methods. Enabling DF for MP2 and CC methods requires explicitly importing the necessary Python modules:

```
from pyscf.mp import dfmp2, dfump2
from pyscf.cc import dfccsd, dfuccsd
mol.RHF().density_fit().run().DFMP2()
mol.UHF().density_fit().run().DFMP2()
mol.RHF().density_fit().run().DFCCSD().run()
mol.UHF().density_fit().run().DFCCSD().run()
```

Besides the post-HF methods, DF can also be used to approximate the orbital Hessian for SOSCF or MCSCF calculations. Although the orbital Hessian is approximated, the energies are still evaluated using the standard integrals. To apply the orbital Hessian for SOSCF, one simply needs to call the `.density_fit()` method of an SOSCF instance, as shown previously (Section IV B). For the CASSCF or state-average CASSCF methods, their `.approx_hessian()` method can be called to approximate the orbital Hessian.

The computational cost and accuracy of the DF approximation are significantly influenced by the quality of the auxiliary basis sets (ABS)^{53,58–60}. Despite the widespread application of DF approximations, the availability of pre-optimized ABS specifically for DF remains limited. For many orbital basis sets (OBS) and quantum chemistry methods, the lack

of specifically optimized ABS is a common issue. To address this issue, several automatic ABS generation schemes have been developed^{61–67}. Schemes like AutoAux⁶⁴ and AutoABS⁶⁶ are available in the PySCF package. Additionally, PySCF maintains a cache of ABS and OBS combinations recommended by the Psi4 package⁶⁸. When the OBS for a particular element is not found in the recommendation cache, PySCF employs an internal ABS generation program to generate even-tempered Gaussian (ETG) basis sets.

In the three-center integrals $(\mu\nu|\chi_P)$, we denote the angular momentum of the two OBS as l_μ and l_ν , and the angular momentum of the ETG ABS as L . The exponent of the Gaussian function within the OBS is represented as α_l , and the exponent of the auxiliary ETG as α_L . For each angular momentum $L = l_\mu + l_\nu$, the PySCF internal ABS generation program determines the minimum exponent

$$\alpha_{L,\min} = \sqrt{\alpha_{l_\mu,\min} \cdot \alpha_{l_\nu,\min}}, \quad (4)$$

and the maximum exponent

$$\alpha_{L,\max} = \sqrt{\alpha_{l_\mu,\max} \cdot \alpha_{l_\nu,\max}}. \quad (5)$$

Here, α_l^{\max} and α_l^{\min} are the maximum and minimum exponents for each angular momentum l of the Gaussian function within the OBS. The exponents for the auxiliary ETG are then generated as

$$\alpha_{L,\min} \cdot 2^n, \quad n = 0, \dots, m \quad (6)$$

The upper bound m is chosen such that $\alpha_{L,\min} \cdot 2^m < \alpha_{L,\max}$.

TABLE I: DF approximation errors for various type of electron repulsion integrals (in Hartree) for the Fe atom in the def2-QZVP basis set.

	universal-jkfit	AutoABS	AutoAux	PySCF built-in
N_{aux}	264	270	550	484
$(ss ss)$	3.77×10^{-4}	0.32×10^{-4}	0.25×10^{-5}	2.06×10^{-5}
$(sp sp)$	2.90×10^{-4}	2.36×10^{-4}	0.32×10^{-5}	2.69×10^{-5}
$(sd sd)$	2.17×10^{-4}	7.59×10^{-4}	0.98×10^{-5}	9.27×10^{-5}
$(sf sf)$	1.58×10^{-3}	11.0×10^{-3}	0.45×10^{-4}	3.61×10^{-4}
$(sg sg)$	1.48×10^{-3}	0.90×10^{-3}	0.31×10^{-4}	2.86×10^{-4}
$(pp pp)$	8.54×10^{-3}	2.68×10^{-3}	1.06×10^{-4}	9.91×10^{-4}
$(pd pd)$	0.12×10^{-2}	6.61×10^{-2}	1.20×10^{-4}	6.80×10^{-4}
$(pf pf)$	2.04×10^{-2}	7.40×10^{-2}	1.14×10^{-4}	8.10×10^{-4}
$(pg pg)$	1.18×10^{-2}	0.516	1.80×10^{-3}	0.67×10^{-3}
$(dd dd)$	0.140	0.0809	0.28×10^{-3}	2.03×10^{-3}
$(df df)$	0.063	2.046	1.05×10^{-2}	0.34×10^{-2}
$(dg dg)$	0.195	0.671	1.39×10^{-2}	0.35×10^{-2}
$(ff ff)$	1.005	2.018	3.88×10^{-2}	3.77×10^{-2}
$(fg fg)$	0.685	1.267	0.657	0.6567
$(gg gg)$	0.566	0.838	0.458	0.4564
total	3.684	12.24	1.866	1.830

Please note that the built-in ABS generation scheme was initially programmed to provide a set of ABS when optimized ABS are not available. However, this scheme is not specifically optimized. The generated ETG basis sets lack functions with large exponents, which may lead to insufficient

Coulomb repulsion between core electrons. Consequently, the electrons experience stronger nuclear attraction, which typically results in a slightly lower electronic energy. In Table I, we display a comparison of errors for the DF approximation using the def2-universal-jkfit⁵³ basis sets, AutoABS, AutoAux, and the PySCF built-in ETG basis sets. The error data shows the differences between the diagonals of the exact integrals and the DF approximate integrals, calculated using the method described by Lehtola⁶³

$$\Delta = \sum_{\mu\nu} \left[(\mu\nu|\mu\nu) - \sum_P T_{P,\mu\nu} T_{P,\mu\nu} \right] \quad (7)$$

The built-in ETG of PySCF is more precise than smaller basis sets such as def2-universal-jkfit or AutoABS. When compared to AutoAux basis sets, they are generally comparable. The PySCF ETG tends to exhibit larger errors. For integrals involving high angular momentum OBS, the accuracy of PySCF ETG is close to or even better than that of AutoAux.

The original ABS generation program is retained in PySCF to maintain backward compatibility. To override the PySCF default ABS management in PySCF, we can assign specifically generated ABS through the keyword argument `auxbasis` when initializing DF methods. For example, the ABS produced by the `autoaux` module can be assigned to DF-DFT calculations as follows:

```
from pyscf.df import autoaux
mf = mol.RKS(xc='pbe0').density_fit(
    auxbasis=autoaux(mol))
```

For larger molecular systems, the DF approximation can become a bottleneck due to computational costs and the storage of the intermediate three-index tensor. At the mean-field level theory, a long-range density fitting (LRDF) scheme⁶⁹ was developed in PySCF to address these challenges. The full-range Coulomb potential can always be written as the summation of the long-range (LR) potential and the short-range (SR) potential

$$\frac{1}{r_{12}} = \underbrace{\frac{\text{erf}(\omega r)}{r_{12}}}_{\text{LR part}} + \underbrace{\frac{\text{erfc}(\omega r)}{r_{12}}}_{\text{SR part}}. \quad (8)$$

The LRDF scheme employs the density fitting technique to approximate the LR Coulomb integrals, while the SR Coulomb integrals are computed exactly:

$$(\mu\nu|\kappa\lambda) \approx (\mu\nu|\kappa\lambda)^{\text{SR}} + \sum_P T_{P,\mu\nu}^{\text{LR}} T_{P,\kappa\lambda}^{\text{LR}}. \quad (9)$$

This request calls for a program to compute the overlap integrals between the absolute values of two orbitals.

$$|S|_{\mu\nu} = \int |\chi_\mu(\mathbf{r})| |\chi_\nu(\mathbf{r})| d\mathbf{r} \quad (12)$$

For Cartesian Gaussian-type orbitals (GTO), this integral can be decomposed into the product of three Cartesian components:

$$|S|_{\mu\nu} = I_x \cdot I_y \cdot I_z. \quad (13)$$

The LR three-index tensor T^{LR} is evaluated with the LR Coulomb metric

$$M_{PQ} = (\chi_P|\chi_Q)^{\text{LR}} = LL^T, \quad (10)$$

$$T_{P,\mu\nu} = \sum_Q (L^{-1})_{PQ} (\chi_Q|\mu\nu)^{\text{LR}}. \quad (11)$$

The computation of the short-range (SR) integrals in Eq. (9) scales linearly with system size. Compared to the full-range Coulomb potential, the rank of the LR integral tensor is substantially lower. One can use a small auxiliary basis set for the LRDF tensor to achieve sufficient accuracy. The size of the auxiliary dimension needed is approximately only 1/10 of the size of the orbital basis functions. This leads to a significant reduction in computational resources and storage. The code example below demonstrates how to apply the LRDF approximation.

```
from pyscf.lrdf import LRDF
mf = mol.RKS(xc='pbe0')
mf.with_df = LRDF(mol)
```

In PySCF 2.9, the LRDF module is available in the PySCF-Forge repository. The PySCF-Forge package must be installed (`pip install pyscf-forge`) before running this example.

V. LEVERAGING MODERN PYTHON TOOLS

The Python community has developed numerous useful tools for scientific programming and numerical computation. Integrating PySCF with these tools can significantly improve the efficiency of theoretical method development and computational simulations. This section presents the use of just-in-time (JIT) compilation, automatic differentiation (AD) to enhance the productivity of PySCF.

A. Just-In-Time (JIT) Compilation

Numba JIT compilation can significantly accelerate Python code by translating Python functions to optimized machine code at runtime. It can be integrated with PySCF functionality to quickly implement features that are not yet available in the package. To illustrate this capability, we will examine a feature request from a PySCF GitHub issue as an example.

Each component is a Gaussian type overlap integral

$$I_x = \int |(x - X_\mu)^{m_x} \exp(-\alpha_\mu(x - X_\mu)^2)| \cdot |(x - X_\nu)^{n_x} \exp(-\alpha_\nu(x - X_\nu)^2)| dx. \quad (14)$$

Given that the exponential component is always positive, the integrands can be rewritten as

$$|(x - X_\mu)^{m_x} (x - X_\nu)^{n_x}| \exp(-\alpha_\mu(x - X_\mu)^2 - \alpha_\nu(x - X_\nu)^2) \quad (15)$$

Employing the Gaussian product theorem, we can simplify the product of two Gaussian functions

$$\exp(-\alpha_\mu(x - X_\mu)^2 - \alpha_\nu(x - X_\nu)^2) = \exp(-\theta_{\mu\nu}(X_\mu - X_\nu)^2) \exp(-(\alpha_\mu + \alpha_\nu)(x - X_p)^2), \quad (16)$$

where

$$\theta_{\mu\nu} = \frac{\alpha_\mu \alpha_\nu}{\alpha_\mu + \alpha_\nu}, \quad (17)$$

$$X_p = \frac{\alpha_\mu X_\mu + \alpha_\nu X_\nu}{\alpha_\mu + \alpha_\nu}. \quad (18)$$

Although I_x appears very similar to the standard Gaussian integral, unless the exponents m_x and n_x are both even, it cannot be analytically computed due to the absolute value of the polynomial. Noting that the integral retains the form of a Gaussian integral, we can approximate it using Gauss-Hermite quadrature, leading to

$$I_x \approx \exp(-\theta_{\mu\nu}(X_\mu - X_\nu)^2) \sum_n w_n |(x_n - X_\mu)^{m_x} (x_n - X_\nu)^{n_x}|. \quad (19)$$

Here, x_n and w_n are transformed from the standard roots u and weights ω of Gauss-Hermite quadrature

$$x_n = \frac{u_n}{\sqrt{\alpha_\mu + \alpha_\nu}} + X_p, \quad (20)$$

$$w_n = \frac{\omega_n}{\sqrt{\alpha_\mu + \alpha_\nu}}. \quad (21)$$

When either m_x or n_x is odd, the polynomial part is not an analytical function and cannot be represented using a finite number of polynomials. To minimize the integral error, a relatively large number of quadratures is required.

The integral code can be easily implemented in Python, as demonstrated in the following example:

```
@numba.njit(fastmath=True, cache=True)
def primitive_overlap(li, lj, ai, aj, ci, cj, Ra, Rb, roots, weights):
    norm_fac = ci * cj
    # Unconventional normalization for Cartesian functions in PySCF
    if li <= 1: norm_fac *= ((li*2+1)/(4*np.pi))**.5
    if lj <= 1: norm_fac *= ((lj*2+1)/(4*np.pi))**.5
    aij = ai + aj
    Rab = Ra - Rb
    Rp = (ai * Ra + aj * Rb) / aij
    theta_ij = ai * aj / aij
    scale = 1./np.sqrt(aij)
    norm_fac *= scale**3 * np.exp(-theta_ij * Rab.dot(Rab))
    x = roots * scale + Rp[:,None]
    xa = x - Ra[:,None]
    xb = x - Rb[:,None]
    mu = xa ** np.arange(li+1)[:,None,None]
    nu = xb ** np.arange(lj+1)[:,None,None]

    nfi = (li+1)*(li+2)//2
    nfj = (lj+1)*(lj+2)//2
    s = np.empty((nfi, nfj))
    i = 0
    for ix in range(li, -1, -1):
        for iy in range(lj-ix, -1, -1):
```

```

iz = li - ix - iy
j = 0
for jx in range(lj, -1, -1):
    for jy in range(lj-jx, -1, -1):
        jz = lj - jx - jy
        Ix = (mu[ix,0] * nu[jx,0] * weights).sum()
        Iy = (mu[iy,1] * nu[jy,1] * weights).sum()
        Iz = (mu[iz,2] * nu[jz,2] * weights).sum()
        s[i,j] = Ix * Iy * Iz * norm_fac
        j += 1
    i += 1
return s

```

The numerical computation workload is intensive in this function. Although NumPy functions already offer a significant speedup compared to plain Python, they are not able to fully utilize CPU capabilities, particularly in terms of using the instruction-level parallelism instructions provided by CPU. Using Numba JIT compilation can accelerate the numerical computation in this integral code.

To generate efficient machine code with Numba JIT, we have enabled the *no-python* mode (`@numba.njit`) in this code example. While the *no-python* mode can produce more efficient machine code for numerical computations, it restricts the use of Python data structures and complex Pythonic features. We are unable to use Python classes or Pythonic iterators within this decorator. Loops and computation expressions have to be written in a straightforward and plain style. In other words, the basis information provided by the PySCF `Mole` class cannot be directly accessed. They have to be converted into simple data representation before being passed the Numba JIT compiled function. This is an inconvenient consequence of using Numba JIT compilation.

The *no-python* compilation mode can leverage more specialized SIMD instructions which might not be supported by NumPy precompiled libraries. This mode automatically employs broader SIMD vectorization, allowing the CPU to execute multiple floating-point operations within a single CPU cycle. This capability is facilitated by the underlying LLVM compiler, which makes Numba JIT-compiled numerical computations faster than NumPy operations in various scenarios. In the `primitive_overlap` function, we have additionally enabled the `fastmath=True` option in the `jit` decorator to activate the FMA (fused multiplication-add) SIMD instructions. The FMA instruction can perform an addition and a multiplication in a single CPU cycle, potentially doubling the performance. However, using FMA can lead to discrepancies compared to performing the multiplication and addition separately^{70,71}. Therefore, it is disabled by default in Numba JIT.

Numba JIT automatically expands NumPy Ufuncs (universal functions) or broadcast operations into loops. However, manually rewriting some of these operations into explicit loops can still benefit computational efficiency. For instance,

the statement

```
mu = xa ** np.arange(li+1)[: ,None,None]
```

can be manually unrolled as

```

for n in range(nroots):
    powx = 1.
    powy = 1.
    powz = 1.
    mu[0,0,n] = 1.
    mu[0,1,n] = 1.
    mu[0,2,n] = 1.
    for i in range(1, li+1):
        powx = powx * xa[0,n]
        powy = powy * xa[1,n]
        powz = powz * xa[2,n]
        mu[i,0,n] = powx
        mu[i,1,n] = powy
        mu[i,2,n] = powz

```

This unrolled version reduces the number of expensive power operations, the number of memory accesses, and the overhead introduced by loops. When calculating I_x , I_y , I_z , the three Ufunc statements are expanded into three loop blocks. We can further optimize this part of the Numba code to reduce the loop overhead and memory footprint, enhancing the overall performance of the simulation.

```

Ix = 0
Iy = 0
Iz = 0
for n in range(nroots):
    Ix += mu[ix,0,n]*nu[jx,0,n]*weights[n]
    Iy += mu[iy,1,n]*nu[jy,1,n]*weights[n]
    Iz += mu[iz,2,n]*nu[jz,2,n]*weights[n]

```

There are several techniques to enhance the performance of Numba JIT. We will not describe each of these optimization techniques in detail in this paper. For a comprehensive discussion, please refer to the dedicated chapters in the book *Python for Quantum Chemistry*⁷².

Subsequently, we invoke the PySCF APIs to gather the necessary information of the GTO functions for this integral function, including angular momentum, exponents, normalization coefficients, and locations. We then iterate over all pairs of GTOs, supplying these data to the integral evaluation function and assemble the output into a matrix:

```

@numba.njit(cache=True)
def primitive_overlap_matrix(
    ls, exps, norm_coef, bas_coords, roots, weights):
    nbas = len(ls)
    dims = [(l + 1) * (l + 2) // 2 for l in ls]
    nao = sum(dims)
    smat = np.empty((nao, nao))
    i0 = 0
    for i in range(nbas):
        j0 = 0
        for j in range(i+1):
            s = primitive_overlap(
                ls[i], ls[j], exps[i], exps[j],
                norm_coef[i], norm_coef[j],
                bas_coords[i], bas_coords[j], roots, weights)
            smat[i0:i0+dims[i], j0:j0+dims[j]] = s
            # smat is a symmetric matrix
            if i != j: smat[j0:j0+dims[j], i0:i0+dims[i]] = s.T
            j0 += dims[j]
        i0 += dims[i]
    return smat

def absolute_overlap_matrix(mol, nroots=500):
    from scipy.special import roots_hermite
    assert mol.cart
    # Integrals are computed using primitive GTOs. ctr_mat transforms the
    # primitive GTOs to the contracted GTOs.
    pmol, ctr_mat = mol.decontract_basis(aggregate=True)
    # Angular momentum for each shell
    ls = np.array([pmol.bas_angular(i) for i in range(pmol.nbas)])
    # need to access only one exponent for primitive gaussians
    exps = np.array([pmol.bas_exp(i)[0] for i in range(pmol.nbas)])
    # Normalization coefficients
    norm_coef = gto.gto_norm(ls, exps)
    # Position for each shell
    bas_coords = np.array([pmol.bas_coord(i) for i in range(pmol.nbas)])

    r, w = roots_hermite(nroots)
    s = primitive_overlap_matrix(ls, exps, norm_coef, bas_coords, r, w)
    return ctr_mat.T.dot(s).dot(ctr_mat)

```

B. Automatic Differentiation

In the realm of automatic differentiation (AD), JAX and Torch are the most commonly used frameworks in Python-based applications. These AD frameworks have been employed in several quantum chemistry-related projects^{9,10,12,14}. Compared to Torch, JAX offers greater flexibility, with highlights in the automatic transitions between the forward-mode (jvp) and backward-mode (vjp) differentiation, the implicit differentiation for fixed-point iterative implementations, and the high-order derivatives. These features make JAX suitable for AD in complex computational programs.

The PySCFAD package developed by Zhang⁹ is a differentiable framework that integrates the AD functionalities of JAX. It offers capabilities for differentiating basis contraction coefficients, the exponents of Gaussian orbitals, and the coordinates of atoms for quantum chemistry methods applicable to both molecular and periodic boundary condition (PBC) systems. The data structure and APIs of PySCFAD are very

similar to those of PySCF. Once the standard (without differentiation) implementation is established in PySCF, adding differentiable functionalities using PySCFAD requires minimal additional effort. As an example, we consider the optimization of auxiliary basis functions for the density fitting method, demonstrating how PySCFAD can be used to compute gradients for newly developed theoretical models.

The density fitting approximation Eq. (1) can be rewritten as

$$(\mu\nu|\kappa\lambda) \approx \sum_{PQ} (\chi_P|\mu\nu)(\mathbf{M}^{-1})_{PQ}(\chi_Q|\kappa\lambda). \quad (22)$$

To enhance the accuracy of the DF approximation, we consider optimizing the exponents α_P of the auxiliary GTO χ_P to minimize the error

$$\sum_{\mu\nu} \left[\sum_{PQ} (\chi_P|\mu\nu)(\mathbf{M}^{-1})_{PQ}(\chi_Q|\mu\nu) - (\mu\nu|\mu\nu) \right]^2. \quad (23)$$

This minimization problem is equivalent to a least-squares fitting problem. The least-squares fitting problem can be solved using the `least_squares` function provided by the SciPy package, which requires input functions to compute the residual

$$\sigma_{\mu\nu} = (\mu\nu|\mu\nu) - C_{P,\mu\nu}(P|\mu\nu), \quad (24)$$

```
def residual(mol, auxmol):
    int4c2e = mol.intor('int2e', aosym='s4').diagonal()
    int3c2e = int3c_cross(mol, auxmol, aosym='s2')
    int2c2e = auxmol.intor('int2c2e')
    return np.einsum('ip,pi->i', int3c2e, np.linalg.solve(int2c2e, int3c2e.T)) - int4c2e
```

To enable the automatic differentiation of the residual function, we make the following modifications:

1. Replace the `mol` and `auxmol` instances with the corresponding ones from PySCFAD;
2. Substitute `numpy` with `jax.numpy`.

The code implementation is demonstrated below. Please note the options `trace_ctr_coeff=False` and `trace_ext=False` are used to instantiating the PySCFAD

```
import jax.numpy as jnp
from pyscfad import gto
from pyscfad.df.incore import int3c_corss
mol = gto.Mole()
mol.atom = '''
O   0.   0.000   0.118
H   0.   0.755  -0.471
H   0.  -0.755  -0.471'''
mol.basis = 'cc-pvdz'
mol.build(trace_ctr_coeff=False, trace_exp=False)

auxmol = gto.Mole()
auxmol.atom = mol.atom
auxmol.basis = auxbasis
mol.build(trace_ctr_coeff=False, trace_exp=True)

def residual(auxmol):
    int4c2e = mol.intor('int2e', aosym='s4').diagonal()
    int3c2e = int3c_cross(mol, auxmol, aosym='s2')
    int2c2e = auxmol.intor('int2c2e')
    return jnp.einsum('ip,pi->i', int3c2e, jnp.linalg.solve(int2c2e, int3c2e.T)) -
    int4c2e

jac = jax.jacfwd(residual)(auxmol)
print(jac.exp) # A vector that stores exponents derivatives
```

and the Jacobian of the residual

$$\frac{\partial}{\partial \alpha_p} \sigma_{\mu\nu\kappa\lambda}. \quad (25)$$

Using PySCF APIs, we construct the residual function for a molecule instance `mol` (holding OBS) and `auxmol` (containing ABS).

`mol` instance. These settings disable the track of derivatives for OBS, as our focus is on optimizing the Gaussian exponents of ABS. For the `auxmol` instance, the `trace_exp` is enabled to track the exponent derivatives. In PySCFAD, the exponents are accessible through the `.exp` attribute of the `auxmol` instance. Their derivatives can be accessed via the `.exp` attribute of the output JAX PyTree class⁷³. We explicitly call `jax.jacfwd` in this example because the size of orbital-pairs are typically much larger than the number of unique exponents in ABS, yielding a tall Jacobian matrix. This Jacobian matrix structure is well-suited for the forward-mode AD.

The residual function and its Jacobian function establish

the main framework for the least-squares minimization prob-

lem. The SciPy least_squares API requires that both the residual and the Jacobian function take a NumPy vector as the input argument and produce a NumPy vector as the output. We would need a few additional wrapper code to adapt to the

SciPy least_squares API. The complete implementation, including problem setup, initialization, adaptation code, and the least_squares fitting, is demonstrated below.

```

import jax.numpy as jnp
from pyscf.df.incore import aux_e2
from pyscfad.gto.mole import setup_exp
from pyscfad.df.incore import int3c_cross

def setup_auxbasis(mol, auxbasis):
    int4c2e = mol.to_pyscf().intor('int2e', aosym='s4').diagonal()
    tril_idx = jnp.tril_indices(mol.nao)

    auxmol = gto.Mole()
    auxmol.atom = mol.atom
    auxmol.basis = auxbasis
    auxmol.build(trace_ctr_coeff=False)
    x0 = auxmol.exp
    _, _, env_ptr, unravel_exp = setup_exp(auxmol, return_unravel_fn=True)

    def f_residual_for_jax(auxmol):
        int3c2e = int3c_cross(mol, auxmol, aosym='s1')[tril_idx]
        int2c2e = auxmol.intor('int2c2e')
        return jnp.einsum('ip,pi->i', int3c2e, jnp.linalg.solve(int2c2e, int3c2e.T)) -
        int4c2e

    # The jacobian is typically a very tall matrix
    jax_jac = jax.jacfwd(f_residual_for_jax)

    def jac(x): # A wrapper to update _env and exp before calling JAX AD
        auxmol._env[env_ptr] = x
        auxmol.exp = jnp.array(x)
        return jax_jac(auxmol).exp

    def f_residual(x):
        auxmol._env[env_ptr] = x
        return f_residual_for_jax(auxmol)

    return f_residual, jac, x0, unravel_exp

if __name__ == '__main__':
    from scipy.optimize import least_squares
    auxbasis = {
        'C': [[0, [9., 1.]],
              [0, [3., 1.]],
              [0, [1., 1.]],
              [1, [3., 1.]],
              [1, [1., 1.]],
              [2, [1., 1.]]],
        'O': [[0, [9., 1.]],
              [0, [3., 1.]],
              [0, [1., 1.]],
              [1, [3., 1.]],
              [1, [1., 1.]],
              [2, [1., 1.]]]
    }
    f_residual, jac, x0, unravel_exp = setup_auxbasis(mol, auxbasis)
    result = least_squares(f_residual, x0, jac=jac, gtol=1e-6, verbose=2)
    print(unravel_exp(result.x))

```

There are several noteworthy aspects in this implementation:

- PySCFAD currently cannot effectively handle the permutation symmetry in the integrals. When calculating the `int3c2e` tensor, the permutation symmetry between orbital pairs (as indicated by `aosym='s1'`) is not utilized. Instead, we compute the entire three-index tensor and extract the unique variables located in the lower triangular part.
- The `least_squares` optimization continuously generate new vectors of exponents. For each new vector, before calling the residual function or the Jacobian function, we need to update the corresponding attributes of `auxmol` to incorporate the new vector. The actual analytical Gaussian integrals are computed by the integral program in PySCF, which reads the exponents from `auxmol._env`. The assignment `auxmol._env[env_ptr] = x` synchronizes the newly generated exponents vector to `auxmol._env`. The addresses `env_ptr` here are obtained via the PySCFAD helper function `setup_exp()`. Additionally, `auxmol.exp` attribute from PySCFAD needs to be updated to post-process the integral differentiations.
- The assignment `auxmol._env[env_ptr] = x` is an operation with side effects and is not JAX transformable. It cannot be placed inside a JAX function. Therefore, we only execute this assignment in the wrapper functions.

If the task is to optimize the even-tempered Gaussian parameters $\alpha_{L,\min}$ and β_L ,

$$\alpha_{L,\min} \cdot \beta_L^n \quad (26)$$

a similar program can be implemented. In this program, an adaptive wrapper function would need to transform the $\alpha_{L,\min}$ and β_L parameters into the PySCFAD `Mole.exp` representation. The adaptation function can be written to comply with JAX-transformable standards, and JAX can easily handle them within the AD framework. More detailed implementation has been documented as an example within the PySCFAD project. For additional information on the technical aspects of JAX AD in the context of quantum chemistry, please refer to the discussions in the book *Python for Quantum Chemistry*⁷⁴.

We then use this program to examine the optimal values for the α_{\min} and β parameters in the auxiliary ETG basis sets. Table II presents the DF approximation errors for some optimized ETG basis sets for the integrals of Fe atom in the def2-TZVP OBS. The error introduced by PySCF built-in ETG is small, implying that its size could potentially be optimized for better performance. Reducing the size of the ETG basis set to smaller ones (ETG I and ETG II) only slightly increase the overall error. In these ETG basis sets, the optimal β values are between 2.0 and 2.2. Even with a reduction of nearly half of the auxiliary basis functions (ETG III), the error remains relatively small. However, the optimal β value would need to be increased to 2.5 or larger.

TABLE II: Optimized ETG parameters for DF auxiliary basis set for the Fe atom in the def2-TZVP basis set.

PySCF built-in ETG							
L	0	1	2	3	4	5	6
n_L	21	17	15	12	10	5	1
$\alpha_{L,\min}$	0.084	0.150	0.124	0.222	0.182	0.763	3.196
β_L	2.0	2.0	2.0	2.0	2.0	2.0	
total error	7.42×10^{-3}						
ETG I							
L	0	1	2	3	4	5	6
n_L	17	14	12	10	8	4	1
$\alpha_{L,\min}$	0.121	0.188	0.157	0.237	0.190	1.152	3.196
β_L	2.200	1.954	2.202	1.953	1.937	2.006	
total error	1.06×10^{-2}						
ETG II							
L	0	1	2	3	4	5	6
n_L	14	11	10	8	6	4	1
$\alpha_{L,\min}$	0.121	0.149	0.157	0.229	0.206	1.223	3.196
β_L	2.196	2.237	2.157	2.113	2.313	1.905	
total error	2.62×10^{-2}						
ETG III							
L	0	1	2	3	4	5	6
n_L	11	9	8	6	5	3	1
$\alpha_{L,\min}$	0.118	0.171	0.117	0.280	0.228	1.085	3.196
β_L	2.982	2.613	2.592	2.544	2.545	2.192	
total error	0.139						

VI. CONCLUSION

In this paper, we have provided a guide for developing and accelerating quantum chemistry program computations using the PySCF framework and modern Python programming tools. We explored various methods to enhance computation performance by manipulating initial guesses, applying second-order convergence, and utilizing integral approximations, through PySCF built-in functionalities. The PySCF extensions, GPU4PySCF and PySCFAD, further enhance the capabilities of the PySCF package. For computationally demanding tasks, the GPU kernels provided by GPU4PySCF offer a straightforward and effective method for acceleration. We demonstrated the use of GPU4PySCF APIs and the coordination between GPU4PySCF and PySCF features. Additionally, Python programming tools can be integrated with the PySCF package to develop new methods and features efficiently. One such example is the use of Numba JIT compilation. By using this tool in conjunction with PySCF's simple APIs, we can optimize CPU resource utilization for numerical computations. We also illustrate the process of using the PySCFAD package to develop automatic derivatives for the exponents of auxiliary Gaussian basis functions in density fitting methods, which are then used in basis set optimization tasks.

VII. ACKNOWLEDGMENTS

The author, Qiming Sun, would like to express his gratitude to Dr. Xing Zhang for helpful discussions on JAX function-

alities and for reviewing the GitHub pull request of additional AD features in PySCFAD related to this work.

- ¹Q. Sun, X. Zhang, S. Banerjee, P. Bao, M. Barbry, N. S. Blunt, N. A. Bogdanov, G. H. Booth, J. Chen, Z.-H. Cui, J. J. Eriksen, Y. Gao, S. Guo, J. Hermann, M. R. Hermes, K. Koh, P. Koval, S. Lehtola, Z. Li, J. Liu, N. Mardirossian, J. D. McClain, M. Motta, B. Mussard, H. Q. Pham, A. Pulkin, W. Purwanto, P. J. Robinson, E. Ronca, E. R. Sayfutyarova, M. Scheurer, H. F. Schurkus, J. E. T. Smith, C. Sun, S.-N. Sun, S. Upadhyay, L. K. Wagner, X. Wang, A. White, J. D. Whitfield, M. J. Williamson, S. Wouters, J. Yang, J. M. Yu, T. Zhu, T. C. Berkelbach, S. Sharma, A. Y. Sokolov, and G. K.-L. Chan, "Recent developments in the pyscf program package," *The Journal of Chemical Physics* **153**, 024109 (2020), https://pubs.aip.org/aip/jcp/article-pdf/doi/10.1063/5.0006074/16722275/024109_1_online.pdf.
- ²D. G. A. Smith, L. A. Burns, D. A. Sirianni, D. R. Nascimento, A. Kumar, A. M. James, J. B. Schriber, T. Zhang, B. Zhang, A. S. Abbott, E. J. Berquist, M. H. Lechner, L. A. Cunha, A. G. Heide, J. M. Waldrop, T. Y. Takeshita, A. Alenaizan, D. Neuhauser, R. A. King, A. C. Simmonett, J. M. Turney, H. F. Schaefer, F. A. Evangelista, A. E. I. I. DePrince, T. D. Crawford, K. Patkowski, and C. D. Sherrill, "Psi4numpy: An interactive quantum chemistry programming environment for reference implementations and rapid development," *J. Chem. Theory Comput.* **14**, 3504–3511 (2018).
- ³K. Boguslawski, A. Leszczyk, A. Nowak, F. Brzęk, P. S. Żuchowski, D. Kędziera, and P. Tecmer, "Pythonic black-box electronic structure tool (pybest): an open-source python platform for electronic structure calculations at the interface between chemistry and physics," *Computer Physics Communications* **264**, 107933 (2021).
- ⁴G. Hermann, V. Pohl, J. C. Tremblay, B. Paulus, H.-C. Hege, and A. Schild, "Orbkit: A modular python toolbox for cross-platform postprocessing of quantum chemical wavefunction data," *J. Comput. Chem.* **37**, 1511–1520 (2016).
- ⁵J. Gao, L. Fu, S. Jiao, Z. Zhang, S. Chen, Z. Zhang, W. Wu, L. Wan, J. Li, W. Hu, and J. Yang, "Pypwdfit: A lightweight python software for single-node 10k atom plane-wave density functional theory calculations," *J. Chem. Theory Comput.* **21**, 2353–2370 (2025).
- ⁶F. A. Evangelista, C. Li, P. Verma, K. P. Hannon, J. B. Schriber, T. Zhang, C. Cai, S. Wang, N. He, N. H. Stair, M. Huang, R. Huang, J. P. Misiewicz, S. Li, K. Marin, Z. Zhao, and L. A. Burns, "Forte: A suite of advanced multireference quantum chemistry methods," *J. Chem. Phys.* **161**, 062502 (2024).
- ⁷M. Chan, T. Verstraelen, A. Tehrani, M. Richer, X. D. Yang, T. D. Kim, E. Vöhringer-Martinez, F. Heidar-Zadeh, and P. W. Ayers, "The tale of horton: Lessons learned in a decade of scientific software development," *J. Chem. Phys.* **160**, 162501 (2024).
- ⁸E. Posenitskiy, V. G. Chilkuri, A. Ammar, M. Hapka, K. Pernal, R. Shinde, E. J. Landinez Borda, C. Filippi, K. Nakano, O. Kohulák, S. Sorella, P. de Oliveira Castro, W. Jalby, P. L. Ríos, A. Alavi, and A. Scemama, "Trexio: A file format and library for quantum chemistry," *J. Chem. Phys.* **158**, 174801 (2023).
- ⁹X. Zhang and G. K.-L. Chan, "Differentiable quantum chemistry with pyscf for molecules and materials at the mean-field level and beyond," *J. Chem. Phys.* **157**, 204801 (2022).
- ¹⁰M. F. Kasim, S. Lehtola, and S. M. Vinko, "Dqc: A python program package for differentiable quantum chemistry," *J. Chem. Phys.* **156**, 084801 (2022).
- ¹¹O. D. Matteo, J. Izaac, T. R. Bromley, A. Hayes, C. Lee, M. Schuld, A. Száva, C. Roberts, and N. Killoran, "Quantum computing with differentiable quantum transforms," *ACM Transactions on Quantum Computing* **4** (2023), 10.1145/3592622.
- ¹²G. Zhou, B. Nebgen, N. Lubbers, W. Malone, A. M. N. Niklasson, and S. Tretiak, "Graphics processing unit-accelerated semiempirical born-ppenheimer molecular dynamics using pytorch," *J. Chem. Theory Comput.* **16**, 4951–4962 (2020).
- ¹³A. S. Abbott, B. Z. Abbott, J. M. Turney, and H. F. I. I. Schaefer, "Arbitrary-order derivatives of quantum chemical methods via automatic differentiation," *J. Phys. Chem. Lett.* **12**, 3232–3239 (2021).
- ¹⁴M. Friede, C. Hölzer, S. Ehlert, and S. Grimme, "dxtb—an efficient and fully differentiable framework for extended tight-binding," *J. Chem. Phys.* **161**, 062501 (2024).
- ¹⁵X. Wu, Q. Sun, Z. Pu, T. Zheng, W. Ma, W. Yan, Y. Xia, Z. Wu, M. Huo, X. Li, W. Ren, S. Gong, Y. Zhang, and W. Gao, "Enhancing gpu-acceleration in the python-based simulations of chemistry frameworks," *WIREs Comput Mol Sci* **15**, e70008 (2025).
- ¹⁶I. Kim, D. Jeong, L. P. Weisburn, A. Alexiu, T. Van Voorhis, Y. M. Rhee, W.-J. Son, H.-J. Kim, J. Yim, S. Kim, Y. Cho, I. Jang, S. Lee, and D. S. Kim, "Very-large-scale gpu-accelerated nuclear gradient of time-dependent density functional theory with tamm-dancoff approximation and range-separated hybrid functionals," *J. Chem. Theory Comput.* **20**, 9018–9031 (2024).
- ¹⁷G. Tornai, I. Ladjánszki, A. Rák, G. Kis, and G. Cserey, "Calculation of quantum chemical two-electron integrals by applying compiler technology on gpu," *J. Chem. Theory Comput.* **15**, 5319–5331 (2019).
- ¹⁸R. Li, Q. Sun, X. Zhang, and G. K.-L. Chan, "Introducing gpu acceleration into the python-based simulations of chemistry framework," *J. Phys. Chem. A* **129**, 1459–1468 (2025).
- ¹⁹G. Vallejo, L. Jorge, C. Snowdon, R. Stocks, F. Kazemian, F. C. Yan Yu, C. Seidl, Z. Seeger, M. Alkan, D. Poole, B. M. Westheimer, M. Basha, M. De La Pierre, A. Rendell, E. I. Izgorodina, M. S. Gordon, and G. M. J. Barca, "Toward an extreme-scale electronic structure system," *J. Chem. Phys.* **159**, 044112 (2023).
- ²⁰S. Seritan, C. Bannwarth, B. S. Fales, E. G. Hohenstein, C. M. Isborn, S. I. L. Kokkila-Schumacher, X. Li, F. Liu, N. Luehr, J. W. Snyder Jr., C. Song, A. V. Titov, I. S. Ufimtsev, L.-P. Wang, and T. J. Martínez, "Terachem: A graphical processing unit-accelerated electronic structure package for large-scale ab initio molecular dynamics," *WIREs Comput Mol Sci* **11**, e1494 (2021).
- ²¹D. Poole, J. L. Galvez Vallejo, and M. S. Gordon, "A new kid on the block: Application of julia to hartree-fock calculations," *J. Chem. Theory Comput.* **16**, 5006–5013 (2020).
- ²²G. J. R. Aroeira, M. M. Davis, J. M. Turney, and H. F. I. I. Schaefer, "Fermi.jl: A modern design for quantum chemistry," *J. Chem. Theory Comput.* **18**, 677–686 (2022).
- ²³W. Wang and J. D. Whitfield, "Basis set generation and optimization in the nislq era with quibox.jl," *J. Chem. Theory Comput.* **19**, 8032–8052 (2023).
- ²⁴Y. Wang, Z. Lin, R. Ouyang, B. Jiang, I. Y. Zhang, and X. Xu, "Toward efficient and unified treatment of static and dynamic correlations in generalized kohn-sham density functional theory," *JACS Au* **4**, 3205–3216 (2024).
- ²⁵F. Neese, F. Wennmohs, U. Becker, and C. Riplinger, "The orca quantum chemistry program package," *J. Chem. Phys.* **152**, 224108 (2020).
- ²⁶C. Peng, C. A. Lewis, X. Wang, M. C. Clement, K. Pierce, V. Rishi, F. Pavošević, S. Slattery, J. Zhang, N. Teke, A. Kumar, C. Masteran, A. Asadchev, J. A. Calvin, and E. F. Valeev, "Massively parallel quantum chemistry: A high-performance research platform for electronic structure," *J. Chem. Phys.* **153**, 044120 (2020).
- ²⁷D. G. A. Smith, L. A. Burns, A. C. Simmonett, R. M. Parrish, M. C. Schieber, R. Galvelis, P. Kraus, H. Kruse, R. Di Remigio, A. Alenaizan, A. M. James, S. Lehtola, J. P. Misiewicz, M. Scheurer, R. A. Shaw, J. B. Schriber, Y. Xie, Z. L. Glick, D. A. Sirianni, J. S. O'Brien, J. M. Waldrop, A. Kumar, E. G. Hohenstein, B. P. Pritchard, B. R. Brooks, I. I. I. Schaefer, Henry F., A. Y. Sokolov, K. Patkowski, I. I. I. DePrince, A. Eugene, U. Bozkaya, R. A. King, F. A. Evangelista, J. M. Turney, T. D. Crawford, and C. D. Sherrill, "Psi4 1.4: Open-source software for high-throughput quantum chemistry," *J. Chem. Phys.* **152**, 184108 (2020).
- ²⁸T. Shiozaki, "Bagel: Brilliantly advanced general electronic-structure library," *WIREs Comput Mol Sci* **8**, e1331 (2018).
- ²⁹D. B. Williams-Young, A. Petrone, S. Sun, T. F. Stetina, P. LeStrange, C. E. Hoyer, D. R. Nascimento, L. Koulias, A. Wildman, J. Kasper, J. J. Goings, F. Ding, A. E. DePrince III, E. F. Valeev, and X. Li, "The chronus quantum software package," *WIREs Comput Mol Sci* **10**, e1436 (2020).
- ³⁰P. O. Dral, "Quantum chemistry in the age of machine learning," *J. Phys. Chem. Lett.* **11**, 2336–2347 (2020).
- ³¹S. Gong, Y. Zhang, Z. Mu, Z. Pu, H. Wang, X. Han, Z. Yu, M. Chen, T. Zheng, Z. Wang, L. Chen, Z. Yang, X. Wu, S. Shi, W. Gao, W. Yan, and L. Xiang, "A predictive machine learning force-field framework for liquid electrolyte development," *Nature Machine Intelligence* **7**, 543–552 (2025).

- ³²Y. Chen, W. Yan, Z. Wang, J. Wu, and X. Xu, "Constructing accurate and efficient general-purpose atomistic machine learning model with transferable accuracy for quantum chemistry," *J. Chem. Theory Comput.* **20**, 9500–9511 (2024).
- ³³D. Khan, A. J. A. Price, B. Huang, M. L. Ach, and O. A. von Lilienfeld, "Adapting hybrid density functionals with machine learning," *Science Advances* **11**, eadt7769 (2025).
- ³⁴J. Wu, S.-M. Pun, X. Zheng, and G. Chen, "Construct exchange-correlation functional via machine learning," *J. Chem. Phys.* **159**, 090901 (2023).
- ³⁵J. Kirkpatrick, B. McMorrow, D. H. P. Turban, A. L. Gaunt, J. S. Spencer, A. G. D. G. Matthews, A. Obika, L. Thiry, M. Fortunato, D. Pfau, L. R. Castellanos, S. Petersen, A. W. R. Nelson, P. Kohli, P. Mori-Sánchez, D. Hassabis, and A. J. Cohen, "Pushing the frontiers of density functionals by solving the fractional electron problem," *Science* **374**, 1385–1389 (2021).
- ³⁶L. Li, S. Hoyer, R. Pederson, R. Sun, E. D. Cubuk, P. Riley, and K. Burke, "Kohn-sham equations as regularizer: Building prior knowledge into machine-learned physics," *Phys. Rev. Lett.* **126**, 036401 (2021).
- ³⁷M. F. Kasim and S. M. Vinko, "Learning the exchange-correlation functional from nature with fully differentiable density functional theory," *Phys. Rev. Lett.* **127**, 126403 (2021).
- ³⁸Q. Sun, T. C. Berkelbach, N. S. Blunt, G. H. Booth, S. Guo, Z. Li, J. Liu, J. D. McClain, E. R. Sayfutyarova, S. Sharma, S. Wouters, and G. K.-L. Chan, "Pyscf: the python-based simulations of chemistry framework," *WIREs Comput Mol Sci* **8**, e1340 (2018).
- ³⁹Q. Sun, "Libcint: An efficient general integral library for gaussian basis functions," *J. Comput. Chem.* **36**, 1664–1671 (2015).
- ⁴⁰C. Li and G. K.-L. Chan, "Accurate qm/mm molecular dynamics for periodic systems in gpu4pyscf with applications to enzyme catalysis," *J. Chem. Theory Comput.* **21**, 803–816 (2025).
- ⁴¹D. S. King and L. Gagliardi, "A ranked-orbital approach to select active spaces for high-throughput multireference computation," *J. Chem. Theory Comput.* **17**, 2817–2831 (2021).
- ⁴²P. Golub, A. Antalik, L. Veis, and J. Brabec, "Machine learning-assisted selection of active spaces for strongly correlated transition metal systems," *J. Chem. Theory Comput.* **17**, 6053–6072 (2021).
- ⁴³Y. Lei, B. Suo, and W. Liu, "icas: Imposed automatic selection and localization of complete active spaces," *J. Chem. Theory Comput.* **17**, 4846–4859 (2021).
- ⁴⁴E. Kolodzeiski and C. J. Stein, "Automated, consistent, and even-handed selection of active orbital spaces for quantum embedding," *J. Chem. Theory Comput.* **19**, 6643–6655 (2023).
- ⁴⁵E. R. Sayfutyarova, Q. Sun, G. K.-L. Chan, and G. Knizia, "Automated construction of molecular active spaces from atomic valence orbitals," *J. Chem. Theory Comput.* **13**, 4063–4078 (2017).
- ⁴⁶J. Zou, K. Niu, H. Ma, S. Li, and W. Fang, "Automatic selection of active orbitals from generalized valence bond orbitals," *J. Phys. Chem. A* **124**, 8321–8329 (2020).
- ⁴⁷J. J. Bao and D. G. Truhlar, "Automatic active space selection for calculating electronic excitation energies based on high-spin unrestricted hartree-fock orbitals," *J. Chem. Theory Comput.* **15**, 5308–5318 (2019).
- ⁴⁸Q. Sun, "Co-iterative augmented hessian method for orbital optimization," (2017), arXiv:1610.08423 [physics.chem-ph].
- ⁴⁹F. Neese, "Approximate second-order scf convergence for spin unrestricted wavefunctions," *Chemical Physics Letters* **325**, 93–98 (2000).
- ⁵⁰L. Thøgersen, J. Olsen, A. Köhn, P. Jørgensen, P. Salek, and T. Helgaker, "The trust-region self-consistent field method in kohn-sham density-functional theory," *J. Chem. Phys.* **123**, 074103 (2005).
- ⁵¹T. H. Fischer and J. Almlöf, "General methods for geometry and wave function optimization," *J. Phys. Chem.* **96**, 9768–9774 (1992).
- ⁵²S. A. Slattery, K. A. Surjuse, C. C. Peterson, D. A. Penchoff, and E. F. Valeev, "Economical quasi-newton unitary optimization of electronic orbitals," *Phys. Chem. Chem. Phys.* **26**, 6557–6573 (2024).
- ⁵³F. Weigend, "Hartree-fock exchange fitting basis sets for h to rn," *J. Comput. Chem.* **29**, 167–175 (2008).
- ⁵⁴T. D. Kühne, M. Iannuzzi, M. Del Ben, V. V. Rybkin, P. Seewald, F. Stein, T. Laino, R. Z. Khaliullin, O. Schütt, F. Schiffmann, D. Golze, J. Wilhelm, S. Chulkov, M. H. Bani-Hashemian, V. Weber, U. Borštnik, M. Tailliefumier, A. S. Jakobovits, A. Lazzaro, H. Pabst, T. Müller, R. Schade, M. Guidon, S. Andermatt, N. Holmberg, G. K. Schenter, A. Hehn, A. Bussy, F. Belleflamme, G. Tabacchi, A. Glöß, M. Lass, I. Bethune, C. J. Mundy, C. Plessl, M. Watkins, J. VandeVondele, M. Krack, and J. Hutter, "Cp2k: An electronic structure and molecular dynamics software package - quickstep: Efficient and accurate electronic structure calculations," *J. Chem. Phys.* **152**, 194103 (2020).
- ⁵⁵R. Li and G. Chan, "Manuscript in preparation on gpu acceleration for multigrid integration algorithm," (2025), manuscript in preparation.
- ⁵⁶X. Zhang and G. Chan, "Manuscript in preparation on multigrid integration algorithm in pyscf," (2025), manuscript in preparation.
- ⁵⁷O. Vahtras, J. Almlöf, and M. W. Feyereisen, "Integral approximations for lcao-scf calculations," *Chemical Physics Letters* **213**, 514–518 (1993).
- ⁵⁸J. G. Hill, "Gaussian basis sets for molecular applications," *Int. J. Quantum Chem.* **113**, 21–34 (2013).
- ⁵⁹K. Eichkorn, O. Treutler, H. Öhm, M. Häser, and R. Ahlrichs, "Auxiliary basis sets to approximate coulomb potentials," *Chemical Physics Letters* **240**, 283–290 (1995).
- ⁶⁰K. Eichkorn, F. Weigend, O. Treutler, and R. Ahlrichs, "Auxiliary basis sets for main row atoms and transition metals and their use to approximate coulomb potentials," *Theoretical Chemistry Accounts* **97**, 119–124 (1997).
- ⁶¹F. Aquilante, L. Gagliardi, T. B. Pedersen, and R. Lindh, "Atomic cholesky decompositions: A route to unbiased auxiliary basis sets for density fitting approximation with tunable accuracy and efficiency," *J. Chem. Phys.* **130**, 154107 (2009).
- ⁶²S. Lehtola, "Straightforward and accurate automatic auxiliary basis set generation for molecular calculations with atomic orbital basis sets," *J. Chem. Theory Comput.* **17**, 6886–6900 (2021).
- ⁶³S. Lehtola, "Automatic generation of accurate and cost-efficient auxiliary basis sets," *J. Chem. Theory Comput.* **19**, 6242–6254 (2023).
- ⁶⁴G. L. Stoychev, A. A. Auer, and F. Neese, "Automatic generation of auxiliary basis sets," *J. Chem. Theory Comput.* **13**, 554–562 (2017).
- ⁶⁵F. Aquilante, R. Lindh, and T. Bondo Pedersen, "Unbiased auxiliary basis sets for accurate two-electron integral approximations," *J. Chem. Phys.* **127**, 114107 (2007).
- ⁶⁶R. Yang, A. P. Rendell, and M. J. Frisch, "Automatically generated coulomb fitting basis sets: Design and accuracy for systems containing h to kr," *J. Chem. Phys.* **127**, 074102 (2007).
- ⁶⁷M. Díaz-Tinoco, R. Flores-Moreno, B. A. Zúñiga-Gutiérrez, and A. M. Köster, "Automatic generation of even-tempered auxiliary basis sets with shared exponents for density fitting," *J. Chem. Theory Comput.* **21**, 2338–2352 (2025).
- ⁶⁸P. Developers, "Psi4 manual: Basis set families," https://psicode.org/psi4manual/master/basissets_byfamily.html#apdx-basisfamily (2025), accessed: 2025-05-29.
- ⁶⁹Q. Sun, "Efficient hartree-fock exchange algorithm with coulomb range separation and long-range density fitting," *J. Chem. Phys.* **159**, 224101 (2023).
- ⁷⁰S. Boldo and J.-M. Muller, "Exact and approximated error of the fma," *IEEE Trans. Comput.* **60**, 157–164 (2011).
- ⁷¹J.-M. Muller, N. Brisebarre, F. de Dinechin, C.-P. Jeannerod, V. Lefèvre, G. Melquiond, N. Revol, D. Stehlé, and S. Torres, "The fused multiply-add instruction," in *Handbook of Floating-Point Arithmetic* (Birkhäuser Boston, Boston, 2010) pp. 151–179.
- ⁷²Q. Sun, "Chapter 9 - program performance optimization," in *Theoretical and Computational Chemistry*, Vol. 23 (Elsevier, 2025) pp. 305–394.
- ⁷³J. Developers, "Jax pytrees documentation," <https://docs.jax.dev/en/latest/pytrees.html> (2025), accessed: 2025-05-29.
- ⁷⁴Q. Sun, "Chapter 16 - molecular properties," in *Theoretical and Computational Chemistry*, Vol. 23 (Elsevier, 2025) pp. 675–712.